IEEE Access
Multidisciplinary ⋮ Rapid Review ⋮ Open Access Journal

Received January 25, 2022, accepted February 7, 2022, date of publication February 14, 2022, date of current version February 23, 2022.

Digital Object Identifier 10.1109/ACCESS.2022.3151379

Fair Power Factor Billing Under Unbalanced and Nonsinusoidal Voltage Supply

VICTOR P. BRASIL, JOÃO Y. ISHIHARA, (Member, IEEE), AND ANÉSIO DE L. FERREIRA FILHO

Electrical Engineering Department, Universidade de Brasília, Brasília 70910-900, Brazil

Corresponding author: Victor P. Brasil (vpradobrasil@gmail.com)

This work was supported in part by the National Council for Scientific and Technological Development (CNPq) under Grant 316487/2021-0, and in part by the Dean of Research and Innovation, that is the "Decanato de Pesquisa e Inovação" (DPI), from the University of Brasília (UnB).

ABSTRACT Utilities apply an additional fee for medium and large customers with low power factors. However, unfair financial charges may occur in installations subjected to voltage unbalance and harmonic distortion. The objective of this paper is to determine the fairest PF definitions and their corresponding measurement algorithms in the case in which a constant impedance load or an induction motor is supplied with unbalanced and nonsinusoidal voltages. Fairness is defined considering that the meter (built based on a particular definition and measurement method) under nonideal supply should lead to very close values as if it was submitted to an ideal balanced sinusoidal supply. We performed computational simulations to emulate several conditions in which a balanced customer (modeled as a constant impedance load or an induction motor) is charged due to a voltage supply no longer balanced and sinusoidal. We also performed experimental tests with an induction motor subjected to a wide range of unbalanced nonsinusoidal supply conditions to ratify the conclusions drawn from the simulations. Based on the simulation results and the experimental tests, we indicate some power factor definitions and measurement methods that are not significantly affected by voltage unbalance and harmonic distortions. These indicated PF definitions provide the fairest billing for conditions with unbalanced nonsinusoidal voltages.

INDEX TERMS Harmonic distortion, induction motor, power factor, voltage unbalance.

I. INTRODUCTION

Under unbalanced and distorted voltage conditions, different power factor (PF) meters may give different readings for the same condition. In [1], it is reported an experience in which an industry's PF dropped from 0.95 to 0.88 after the meter replacement. The new meter would have led to a 4% surcharge in the customer's bill had the technician not noticed this discrepancy. One thing that stands out is that these meters were approved for commercialization and usage. As pointed out by [1], "Utilities must be able to install any meter in any electrical environment (sinusoidal or nonsinusoidal) with full confidence that they will all give the same readings for the same load. Anything less is unacceptable." To achieve such level of confidence, it is necessary to understand the possible causes for measurement divergences.

According to [2], the discrepancies shown in [1] were due to different PF definitions and measurement methods implemented in the commercial meters. It can be noted that although the arithmetical, geometrical (vectorial), positive sequence, and effective PFs discussed in IEEE Standard 1459 [3] give the same value in balanced sinusoidal conditions, it turns out that they may provide different values in unbalanced nonsinusoidal conditions.

The problem of finding a 'correct' general PF definition and measurement method is not a trivial task, and an indication of the most appropriate for each application is still lacking. Most of the countries studied by [4] "have not yet established rules for reactive power billing under nonsinusoidal conditions and keep applying old regulation to systems where voltage and current are not sinusoidal anymore."

As field research, reference [5] investigated the arithmetic, geometric, effective, fundamental, and modified fundamental PF applied to an arc furnace of a real industry in Taiwan. The authors showed that the selection of different definitions can cause an impact up to 1% in the customer's bill. Although this percentage may seem small, it represents a huge impact for large customers with expensive monthly revenues. However, the study of [5] is restricted to industries that use arc furnaces, and it does not consider different supply conditions and measurement methods.

On the other hand, reference [4] compared the fundamental reactive power (Q_1) and the non-active power (N) under several supply conditions and with different measurement

The associate editor coordinating the review of this manuscript and approving it for publication was Md. Rabiul Islam.

methods. Digital simulations were performed to find out which definition is the fairest for billing purposes of a residential load (at 9 pm and 12 pm) under nonsinusoidal voltage supply. According to [4], the definition less sensible to the voltage harmonic distortion is the fairest one, which in their simulations was Q_1. It is also pointed out that Q_1 can be measured with simple digital techniques. The analysis, however, was restricted to a residential load supplied by nonsinusoidal voltages, and it did not consider unbalanced conditions.

Among all PF definitions, the most important seems to be the effective PF (PF^e). In fact, it has been investigated by several researchers [3], [6]–[11] and it is recommended by IEEE Standard 1459-2010 [3] for unbalanced sinusoidal conditions. For unbalanced nonsinusoidal conditions, references [9], [10], [12], [13] ratify PF^e as a measure of the energy transmission efficiency. Furthermore, reference [6] showed that PF^e values of balanced constant impedance loads are not significantly affected by voltage unbalance.

From the foregoing discussion, it can be noticed that evaluation of one important load has not been done yet. According to [14]: ''there are 85 million large electrical motors in the community market. These consume 65–70% of the energy used within industry.'' Therefore, the evaluation of PF billing fairness for balanced three-phase induction motors (TIMs) under unbalanced nonsinusoidal supply voltages is an important issue.

The objective of this paper is to seek the fairest PF definitions and their corresponding measurement algorithms for metering the PF of a balanced customer (modeled as a constant impedance load or an induction motor) submitted to a wide range of unbalanced and nonsinusoidal voltage conditions. Here, the fairness notion is in the sense that the meter (built based on a particular definition and measurement method) under nonideal supply should lead to very close values as if it was submitted to an ideal balanced sinusoidal supply. First, the sensitivity of the main PF definitions (the fundamental geometric, fundamental arithmetic, etc.) with respect to the voltage unbalance is evaluated. Once the fairest PF definitions are identified, the effect of the measurement algorithm on the final value is then assessed.

This paper has the following contributions:

i) It shows that a PF definition that leads to a fair billing for a constant impedance load may not provide a fair billing for a TIM in unbalanced and nonsinusoidal voltage conditions (UNVC).
ii) It determines the fairest power factor (PF) definitions and their corresponding measurement algorithms for metering the PF of any of the two loads, a balanced constant impedance and a TIM, submitted to a wide range of UNVC.

This paper is organized as follows. For a prospect of current standards, representative PF charging policies applied in the real world are revisited in Section II. In Section III, some definitions and measurement methods are listed. Considering the fairness perspective, these PF definitions are evaluated employing computational simulations in Section IV and experimental tests in Section V. In Section VI, measurement techniques for the fairest definitions are evaluated under several unbalanced and nonsinusoidal voltage conditions. At last, conclusions are drawn, and suggestions for future works are given in Section VII.

II. PROSPECT OF PF CHARGING POLICIES

It is a common practice for utilities to adopt mechanisms to encourage customers to control their reactive energy consumption. One of these mechanisms is the PF charging, which consists of financially penalising customers with PF below the established limit. In order to provide a basic overview of the existing charging policies, standards taken from 6 utilities, 9 states, and from 5 countries are investigated and presented in this section. The standards were selected based on different policies adopted worldwide, as presented in [4] and [15]. Results are shown in Table 1.

In Table 1, four types of charging policies are observed. BC-Hydro, for example, applies a surcharge percentage proportional to the PF deviation from the minimum accepted value [16]. Hydro-Quebec, on the other hand, charges the maximum power demand, defined as the greatest value between the maximum real power and 90% of the maximum apparent power [17]. The third and fourth policies are the charging of exceeding reactive power and energy, respectively.

From Table 1, it can be noticed that there is a PF limit/threshold below which charges are applicable, regardless of the policy adopted. In the case of BC-Hydro [16] and Brazilian utility companies [29], the PF should also be used to compute the charge that will be applied.

All investigated standards have explicit statements establishing that residential customers are not chargeable [16]–[30]. This can also be inferred from Table 1 based on the minimum demand[1] above which PF evaluation is applied. The minimum demand threshold (among the investigated standards) found in this investigation was 35 kW, which is not compatible with residential and small customers. Such demand level is typical of medium and large units (in general, industries) supplied by three-phase voltages. Therefore, a three-phase PF definition compatible with the characteristics of TIMs (industries main load [14]) might be more suitable for billing. Nonetheless, it was not found an explicit statement in the investigated documents about which of the existing PF definitions should be used.

Considering the foregoing discussion, it can be concluded that the PF is used as a trigger in all four policies, and, in some of them, it is also used in the computation of the charge. This initial analysis highlights that only medium and large customers are subjected to PF billing. For this reason, the usage of TIMs for evaluating different PFs may be more suitable than the constant impedance load model usually adopted in PF studies. Additionally, it is pointed out the lack of an explicit standardization of which definition should be used for revenue purposes in the investigated standards.

[1]Some standards adopt the average consumption over given periods instead of the instantaneous demand.

TABLE 1. PF legal and regulatory aspects in selected utility companies.

Policy	Country	States	Utility	Minimum Demand or Average Consumption	Minimum Lagging	Minimum Leading	References
Surcharge over the total bill	Canada	British Columbia	BC-Hydro	35 kW	0.9	Not regulated	[16]
Charge "maximum power demand"		Quebec	Hydro-Quebec	65 kW	0.9 (0.95 for large customers with 5 MW or more)	Not allowed	[17]
Charge reactive power	Australia	Victoria	All	150 kVA	[0.75; 0.95] depending on demand and voltage level	[0.8; 0.98] depending on demand and voltage level	[18]
		Queensland	Ergon Energy's	4 GWh per year	0.8	Allowed only in specific cases	[19], [20]
		Western Australia	Synergy	1285 kWh per day	0.8	Not allowed	[21], [22]
Charge reactive energy	England	Southern Electric	Southern Electric Power Distribution	100 kW	0.95		[23]–[25]
	Scotland	Merseyside, North Wales, South Scotland	Scottish Power				[25]–[27]
Charge reactive energy or power	Brazil	All	All	112.5 kVA	0.92	0.92	[28]–[30]

III. POWER FACTOR DEFINITIONS AND MEASUREMENT METHODS

In this section, we recall some definitions and measurement methods presented by IEEE standard 1459-2010 [3]. The advantages and disadvantages of the measurement methods, as well as the signal processing requirements, can be found in [3].

In sinusoidal balanced systems, the energy transmission efficiency (or line utilization) can be measured by the PF which can be computed in terms of the total active power (P) and apparent power (S) as [3], [31]

$$PF = \frac{P}{S}, \tag{1}$$

where P and S are computed by the classical theory of alternate current (AC) polyphase systems [3], [31]. Alternatively, the reactive power (Q) can be used to compute the PF as

$$PF = \frac{P}{\sqrt{P^2 + Q^2}}. \tag{2}$$

Under these conditions, low transmission efficiency is related uniquely to the reactive power flow.

The presence of voltage unbalance and/or harmonic distortion contribute to lower the transmission efficiency. In this case, there is no consensus on the meaning and definition of reactive power, apparent power and PF, as can be observed in [3], [6], [8]–[12], [32]–[39]. Some of the several PF definitions proposed in the literature are provided in [3]. These definitions can be divided according to the phenomenon they address: i) harmonic distortion, ii) voltage unbalance, and iii) the concurrence of i) and ii).

In nonsinusoidal single-phase systems, the single-phase 'true' apparent power[2] (S_T) can be decomposed accordingly to Fryze [33] or to Budeanu [34]. In both cases, S_T is computed as

$$S_T = V_T I_T \tag{3}$$

where V_T and I_T refer to the true RMS values of voltage and current, respectively. According to Fryze, S_T is decomposed as

$$S_T = \sqrt{P^2 + N^2} \tag{4}$$

where N is the non-active power. In Budeanu's approach, S_T is broken into

$$S_T = \sqrt{P^2 + Q_B^2 + D_B^2} \tag{5}$$

where Q_B and D_B are Budeanu's reactive and distortion power, respectively. At this point, divergences regarding PF starts. For instance, some meters employ (3) in (1), while others compute the PF via (2) considering the reactive power equal either to N or to Q_B.

In [3], decomposition of S_T in terms of the fundamental apparent power (S_1) and the nonfundamental apparent power (S_N) is presented. With S_1, the fundamental power factor (PF_1) is defined as

$$PF_1 = \frac{P_1}{S_1} \tag{6}$$

where P_1 is the fundamental active power.

In balanced nonsinusoidal systems, all phases have the same PF value if the same definition is employed. In this case, the load PF is exactly equal to the PF measured in any of the phases. The only cause for possible divergences is due to different single-phase definitions (usage of N or Q_B for instance).

In sinusoidal unbalanced systems, any definition used to compute the PF per phase will give exactly the same results. However, phases will have different PF values. Some

[2]This is called 'true' apparent power because it is computed from the true RMS values of voltage and current as in (3).

approaches to obtain the load PF are to compute it arithmetically or geometrically, which are respectively given by

$$PF^a = \frac{P}{S_A + S_B + S_C} \tag{7}$$

$$PF^g = \frac{P}{\sqrt{P^2 + Q^2}}, \tag{8}$$

where Q is the three-phase reactive power, computed by the sum of each phase reactive power, and S_X is the apparent power for phase $X = A, B, C$. It is noteworthy that different reactive and apparent power definitions can be employed in (7) and (8), which can result in different values under nonsinusoidal conditions.

Alternatively, the load PF can be adopted as the positive sequence PF (PF^+) given by

$$PF^+ = \frac{P^+}{S^+}. \tag{9}$$

Since the positive sequence system is completely balanced, S^+ can be computed as $S^+ = S^{+a}$ or $S^+ = S^{+g}$ in which

$$S^{+a} \triangleq S_A^+ + S_B^+ + S_C^+, \tag{10}$$

and

$$S^{+g} \triangleq \sqrt{\left(P^+\right)^2 + \left(Q^+\right)^2}. \tag{11}$$

Setting $S^+ = S^{+a}$ or $S^+ = S^{+g}$ in (9) leads respectively to the positive sequence arithmetical power factor

$$PF^{+a} = \frac{P^+}{S^{+a}} \tag{12}$$

and to the positive sequence geometrical power factor

$$PF^{+g} = \frac{P^+}{S^{+g}}. \tag{13}$$

The quantities PF^{+a} and PF^{+g} are mathematically equivalent ($PF^{+a} = PF^{+g}$) but may have different values depending on the chosen measurement method. [3] Since this section deals only with definitions, the positive sequence will be simply denoted by PF^+.

It is also possible to employ the effective power factor (PF^e) computed as

$$PF^e = \frac{P}{S^e} \tag{14}$$

$$S^e = 3\, V^e I^e \tag{15}$$

where V^e and I^e are the effective voltage and current respectively. In terms of symmetrical sequence components, they are computed as

$$V^e = \sqrt{\left(V^+\right)^2 + \left(V^-\right)^2 + \frac{\left(V^0\right)^2}{1+\xi}} \tag{16}$$

[3]The apparent power $S_X^+, X = A, B, C$ can be measured based on the RMS values of positive sequence voltage and current of each phase, whereas S^{+g} requires the measurement of active and reactive power. The methods for measuring the voltage and current RMS values are different from those used to measure the active and reactive power. As a result, the measurements of PF^{+a} and PF^{+g} may have different values.

TABLE 2. Possible three-phase PF definitions.

	Fundamental	Non-Active Power (Fryze)	Budeanu's Reactive Power	Effective
Arithmetic	PF_1^a	PF_N^a	PF_B^a	-
Geometric	PF_1^g	PF_N^g	PF_B^g	-
Effective	-	-	-	PF^e
Positive Sequence	PF_1^+	PF_N^+	PF_B^+	-

$$I^e = \sqrt{\left(I^+\right)^2 + \left(I^-\right)^2 + (1+3\rho)\left(I^0\right)^2}, \tag{17}$$

where V^+, V^-, and V^0 are the positive, negative, and zero sequence voltage true RMS values, respectively. Analogously, I^+, I^- and I^0 refers to the currents sequence components true RMS values. The variables ξ and ρ are used to consider the effects of zero sequence components in the system. If ξ and ρ are unknown, it is recommended to set them to one [3].

The possible combinations of single-phase quantities with the aggregation method to compute the load PF results in the definitions shown in Table 2. Each row is a method to aggregate single-phase values and to calculate the load PF. The columns refer to definitions under nonsinusoidal conditions. It is worth mentioning that the effective power factor cannot be combined with different definitions because it is already uniquely defined for both unbalanced and nonsinusoidal conditions.

The effectiveness of a PF measure depends on the definition employed and on the implemented measurement method. Therefore, in the following subsections, we select some measurement algorithms to be presented.

A. ACTIVE POWER MEASUREMENT METHODS

It is known that the total three-phase active power is obtained by adding up the total active power of each phase. According to [3], the total active power, in balanced nonsinusoidal conditions, can be decomposed into fundamental active power (P_1) and total harmonic active power (P_H).

In the general case, where voltage unbalance and harmonic distortion can be present, these last two decompositions can be superimposed resulting in 6 components: $P_1^+, P_1^-, P_1^0, P_H^+, P_H^-$ and P_H^0.

The total active and positive sequence powers are measured, respectively, by [3]

$$P \approx \sum_{X=A,B,C} \frac{1}{kT} \int_t^{t+kT} v_X(t) i_X(t) dt \tag{18}$$

$$P^+ \approx 3\frac{1}{kT} \int_t^{t+kT} v_A^+(t) i_A^+(t) dt, \tag{19}$$

where $v_X(t)$ and $i_X(t)$ are the voltage and current from phase $X = A, B, C$; $v_A^+(t)$ and $i_A^+(t)$ are the positive sequence voltage and current of phase A; T is the signal period, and k is the total number of cycles measured.

B. REACTIVE POWER MEASUREMENT METHODS

The methods of voltage integration and of 90° displacement of voltage, based on voltage and current instantaneous samples, are defined as follows.

1) 90° DISPLACEMENT OF VOLTAGE [40]

Reactive power per phase is computed applying a 90° shift via time delay to the voltage of that phase as

$$Q_{X,\text{displacement}} = \frac{1}{T}\int_0^T v_X\left(t-\frac{T}{4}\right)\cdot i_X(t)dt. \quad (20)$$

2) VOLTAGE INTEGRATION [41]

The reactive power is estimated using a 90° phase shift in sinusoidal signals obtained from integration as follows

$$Q_{X,\text{integration}} = \frac{\omega}{T}\int_0^T \left[\int v_X(t)dt\right]\cdot i_X(t)dt. \quad (21)$$

According to [4], $Q_{X,\text{displacement}}$ and $Q_{X,\text{integration}}$ can be considered approximately equal to Q_{1X} under common distortion levels.

Besides the two mentioned measurement algorithms, there is a wide range of algorithms inspired by different techniques. They are based on voltage and current instantaneous samples, on phasor measurements, on the fast Fourier transform (FFT), and on the wavelet transform [40], [42]–[44]. In this work, we present only the simpler measurement algorithms (the 90° shift and voltage integration), which are sufficient for the precision evaluation of the fairest PF definitions, as corroborated by the experiments in Section VI.

C. POSITIVE SEQUENCE POWER MEASUREMENT ALGORITHMS

It is known that performing FFT is computationally costly and that physical filters have limitations [45]–[47]. Therefore, this section shows a simple method for measuring the fundamental positive sequence geometrical PF (PF_1^{+g}).

First, the phase A voltage instantaneous positive sequence component is extracted with the proposed algorithm of [48] as follows,

$$v_A^+(t) = \frac{1}{3}\left[v_A(t) + v_B\left(t-\frac{2T}{3}\right) + v_C\left(t-\frac{T}{3}\right)\right]. \quad (22)$$

The instantaneous positive sequence current $i_A^+(t)$ is extracted analogously. Then, it is assumed that P_1^+ is approximately equal to P^+, which is computed by (19). The fundamental positive sequence reactive power (Q_1^+) is estimated with the 90 degree displacement of voltage (20) or the voltage integration (21) methods substituting $v_X(t)$ and $i_X(t)$ by $3v_A^+(t)$ and $3i_A^+(t)$. Having computed P_1^+ and Q_1^+, the value of PF_1^{+g} is obtained by

$$PF_1^{+g} = \frac{P_1^+}{\sqrt{(P_1^+)^2+(Q_1^+)^2}}. \quad (23)$$

TABLE 3. TIM equivalent circuit parameters at 60 Hz.

Parameter	R_S	R_r	X_S	X_r	X_m
Value (Ω)	0.294	0.144	0.503	0.209	13.25

IV. EVALUATION OF DIFFERENT POWER FACTOR DEFINITIONS FROM THE FAIRNESS PERSPECTIVE

To quantify the impacts of adopting different definitions for billing purposes, in this section, we evaluate all possible PF definitions presented in Section III.

For this purpose, simulations of two balanced, linear, constant loads with the reference PF ($PF_{\text{ref.}}$) equal to 0.95 are performed considering different unbalanced nonsinusoidal voltages. The $PF_{\text{ref.}}$ is defined under balanced sinusoidal conditions. Thus, it can be computed by any definition.

One of the loads employed is a constant impedance, following the literature trend [3], [6], [8]–[12]. A delta connection is used, and the reference PF is set by declaring each individual impedance branch with an angle of $\cos^{-1}(0.95)$.

The second load selected was a TIM because, in the studied countries, PF billing applies for medium and large consumers. Since the TIM represents approximately 65–70% of industries' total consumption [49], it is important to observe how PF definitions affect this specific load. The simulated TIM is delta connected, 220 V (line-to-line), 7.5 kW, 60 Hz and has six poles. It is modeled accordingly to [50], [51] with the electrical parameters shown in Table 3. A constant slip of 1.5% is adopted, representing medium loading. Additionally, to emulate real operating conditions, the motor reactive power is partially compensated by delta connected capacitors so that its PF_{ref} is equal to 0.95.

Several supply conditions are evaluated to identify the effects of each voltage parameter on the existing PF definitions. All combinations of $V^+ \in [0.9, 1.1]$ pu in steps of 0.05 pu and of V^- and $V^0 \in [0, 0.03]$ pu in steps of 0.005 pu are considered. These magnitudes were chosen so that the positive sequence is never greater or less than 10% of the nominal voltage and so that the maximum voltage unbalance factor (VUF), given by

$$\text{VUF} = \frac{V^-}{V^+}, \quad (24)$$

is below 3.5%, which is slightly higher than the VUF usual limits in existing regulations [28], [52]. The angles θ^0 and θ^- used in the database range from 0 to 330° in steps of 30°. The angle θ^+ is selected as the angular reference. Thus, it is set to zero in all cases. The voltage harmonics described in Table 4 are superimposed proportionally to each of the system unbalanced voltages, resulting in a total harmonic distortion (THD) of 3.74%. According to [4], the third, fifth and seventh harmonics components (with their magnitude and angle values presented in Table 4) are typical for voltage distortions in power systems. Proceeding in this way, a total of 35280 voltage conditions are simulated.

It is noteworthy that the simulated conditions result in VUF values in the range of 0 up to 3.5% approximately. These values of VUF are close to those found in some distribution

TABLE 4. Voltage harmonics.

Harmonic order	1	3	5	7
Magnitude [% of nominal]	100	2	3	1
Angle [degrees]	0	70	−90	−145

systems, and to the limits established by some standards. In fact, a voltage unbalance between 1% and 3% is present in 32% of the distributions systems in the United States, according to [52]. In terms of standards, the European Standard EN 51060, for example, establishes that the VUF should be lower than 2% in 95% of 10 minutes periods, according to [52].

A. PER PHASE POWER FACTOR

In the lack of a PF definition for billing purposes, a per phase approach may seem reasonable since the customer can act and compensate each phase individually.

1) CONSTANT IMPEDANCE LOAD

A set of different supply conditions was first applied to the constant impedance load, which was held constant by keeping its magnitude constant. Since the load is connected in delta, line voltages (measured between phases) were employed to compute $PF_{1X}, X = A, B, C$.

From the results obtained, it is possible to conclude that, for all investigated conditions, the computed $PF_{1X}, X = A, B, C$ was constant and equal to the reference value of 0.95. The same conclusion was found by [6] using different voltage conditions.

2) THREE-PHASE INDUCTION MOTOR

Afterwards, the dataset was applied to the TIM. It should be highlighted that the motor is considered to operate a mechanical load with constant speed. As a result, the motor slip is set to 1.5% for all VU conditions. Since the desired mechanical output is constant and the motor is not modified, except for the voltages applied in it, the load can be characterised as constant from the customer's perspective. Consequently, its PF should also be constant.

Fig. 1 shows a scatter plot of PF_{1A} as a function of the VUF for all 35280 conditions of the database. Many of these conditions result in the same pair of VUF and PF values, leading to the superimposition of points in the graph. Similar results are obtained for the remaining phases, which are not shown to avoid graph cluttering. From Fig. 1, it can be observed that PF_{1A} can have different values for the same VUF. For instance, a 1.5% VUF results in PF_{1A} ranging from 0.88 up to 0.99. For a VUF of 3%, there are conditions that lead to PF_{1A} values in between 0.8 lagging up to 0.999 leading. Therefore, it can be concluded that the interval of possible values for PF_{1A} increases with the VUF.

Although the results for phases "B" and "C" are analogous to those presented for phase "A" in Fig. 1, it was observed that each phase had a different behaviour for each VU condition. Two different conditions that yields 1% VUF can result in different $PF_{1X}, X = A, B, C$ values, as shown in Table 5. In order to assess the VUF associated with conditions that cause charges in at least one of the phases, the minimum fundamental PF between phases ($PF_{1\text{min}}$) for each condition is computed and shown in Fig. 2.

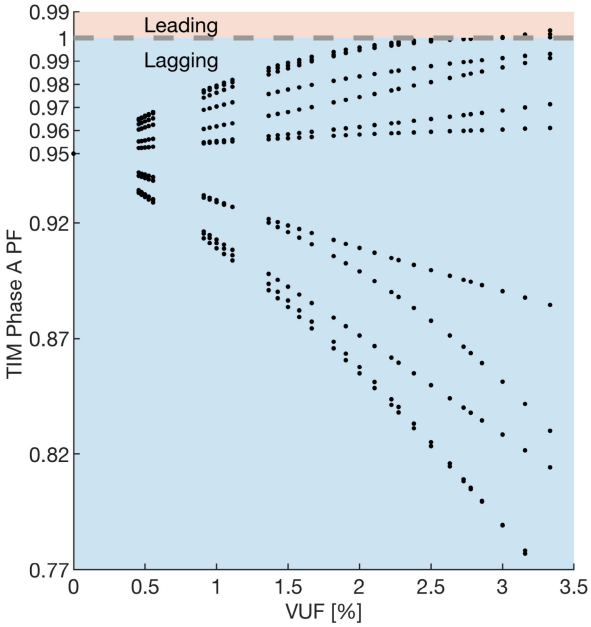

FIGURE 1. TIM PF_{1A} as a function of VUF, with a THD of 3.74%.

TABLE 5. TIM power factor per phase for two conditions.

Condition	PF_{1A}	PF_{1B}	PF_{1C}
$V_1 = 1\angle 0$ $V_2 = 0.01\angle 0$	0.91	0.97	0.96
$V_1 = 1\angle 0$ $V_2 = 0.01\angle 30°$	0.96	0.97	0.91

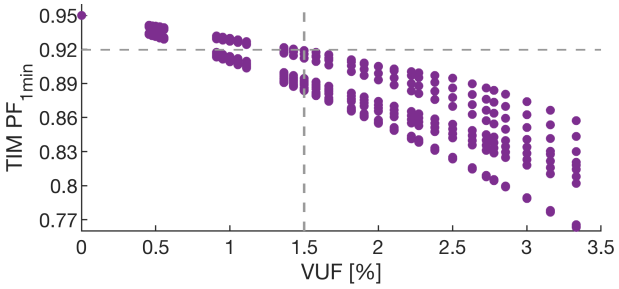

FIGURE 2. TIM $PF_{1\text{min}}$ as a function of VUF, with a THD of 3.74%.

Similarly to PF_{1A} shown in Fig. 1, there are conditions with the same VUF that leads to different values of $PF_{1\text{min}}$ as shown in Fig. 2. The range of possible values also increases with the VUF. From Fig. 2, it can be observed that for a VUF of 1% there are some conditions conducting to values of $PF_{1X}, X = A, B, C$ lower than 0.92 in at least one of the phases. For VUF equal or greater than 1.5%, all simulated conditions yielded at least one phase $PF_{1X}, X = A, B, C$ lower than the commonly acceptable value of 0.92. In both situations, the VUF is still within the usually acceptable limit of 2% [52], and the utility has no obligation to improve the supply quality. Nonetheless, the existing unbalance in the grid

may result in PF charges if a per phase charging is applied or if $PF_{1\text{min}}$ is utilized as the three-phase PF definition.

Summarizing, both the per phase approach as well as $PF_{1\text{min}}$ are highly sensitive to the VU. For a given VUF, there are several conditions yielding different PF values. Some conditions can even result in leading PF, which is unacceptable in some regulations as shown in Section II. Moreover, when the VUF is equal or greater than 1.5%, at least one of PF_{1X}, $X = A, B, C$ is less than 0.92. What stands out is that the customer's load was held constant with PF_{ref} equal to 0.95 under balanced conditions. Therefore, these approaches are not suitable for billing purposes neither for constant impedance loads nor for TIMs.

B. THREE-PHASE POWER FACTOR

Given that PF computed per phase is not suitable for billing purposes, three-phase definitions are investigated for a constant impedance load and for the induction motor.

In [4], [37], [53], fairness aspects of some three-phase definitions have been discussed under unbalanced and nonsinusoidal conditions. The issues regarding Budeanu's power definitions are extensively pointed out in [53] and [37]. Investigating nonsinusoidal conditions, the authors of [4] concluded that usage of fundamental quantities, instead of quantities based on the non-active power, are fairer for billing purposes. Therefore, the definitions presented in the columns of Table 2 related to Budeanu's reactive power and non-active power are also not suitable for billing purposes. With this, PF_1^g, PF_1^a, PF_1^+ and PF^e are evaluated in this study considering the same 35280 conditions used in simulations of Section IV-A. For the computation of PF^e, the values of ξ and ρ in (16) and in (17) are set to one, following the recommendation given in [3] when they are unknown.

1) CONSTANT IMPEDANCE LOAD

For the constant impedance load submitted to VUF up to 3.4%, it was observed that PF_1^g and PF_1^+ are always equal to the PF_{ref}, while PF_1^a and PF^e presented more variation around PF_{ref} but still with standard deviation less than 10^{-4}.

2) THREE-PHASE INDUCTION MOTOR

Fig. 3 shows the scatter plot for each definition computed for the TIM against the respective VUF associated with the supply condition. First, it should be noted that for balanced conditions, PF_1^a, PF_1^g, PF^e and PF_1^+ are equal to the reference value of 0.95. For unbalanced conditions, it can be observed that PF_1^a and PF^e values are lower than PF_{ref}. For unbalance close to 2.5%, their values are lower than 0.92, and the customer may be penalised. Differently from PF_1^g, PF^e and PF_1^+, the definition PF^a can have different values for the same VUF. So, neither PF^a nor PF^e are suitable for billing purposes given their sensitivity to the VU. On the other hand, both PF_1^g and PF_1^+ are approximately constant and equal to PF_{ref}. Therefore, PF_1^g and PF_1^+ are recommended for revenue purposes.

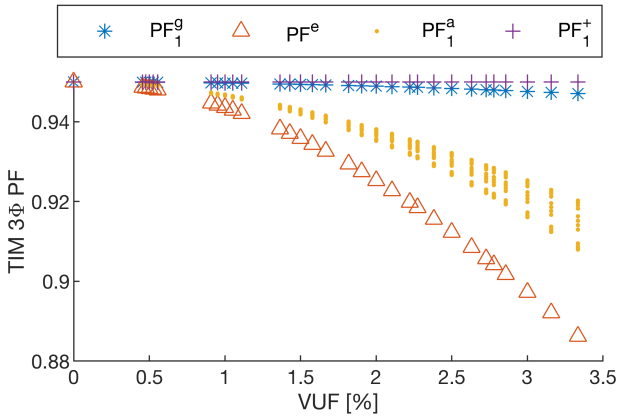

FIGURE 3. Different 3ϕ PF definitions computed for the TIM as a function of the VUF with simulated data (THD of 3.74%).

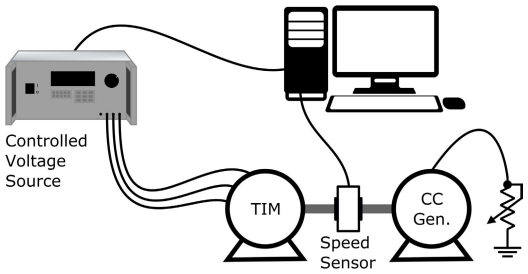

FIGURE 4. Connections of the equipment used in the experimental setup.

The authors are aware that unbalanced loads may cause voltage unbalance. In these simulations, however, the loads were perfectly balanced and kept constant so that the customer had no responsibility for the supply quality.

V. EXPERIMENTAL EVALUATION OF POWER FACTOR DEFINITIONS

In this section, the sensitivity to the voltage unbalance of different PF definitions is evaluated experimentally with a motor operating under unbalanced and distorted voltages. The experimental setup consists of a controlled voltage source (California Instruments CSW 11110), a speed sensor, a 4 kW DC generator, a variable resistor, and a 1,5 kW three-phase squirrel cage induction motor (4 poles, 60 Hz, rated 220 V and connected in delta).

The CSW 1110 supplies the motor with unbalanced and nonsinusoidal voltages. The motor drives the DC generator, which feeds the variable resistor. The DC generator and the variable resistor, working together, emulate a mechanical load in the motor shaft. The variable resistor is adjusted so that the motor operates with nominal power. A speed sensor is used to check if the motor speed was constant throughout the experiment. The connections between the equipment are shown in Figure 4.

To confirm that the conclusions drawn from the simulations study are not particular for the set of supply conditions and the motor considered, the experimental PFs were evaluated at different supply conditions (another collection of VUF values, harmonic spectra, and distortion levels) applied to another TIM operating close to nominal power. In the

construction of the set of unbalanced supply conditions, the following values are taken into consideration: $V^+ \in [0.87, 1.06]$ pu in steps of 0.02 pu, VUF $\in$ [0, 4]% in steps of 0.5% and $\theta^- \in [0°, 120°]$ in steps of 24°. All these values are combined, forming a set of 442 voltage conditions. For the harmonics, it is considered the pairs of harmonics: (third, fifth), (third, seventh), and (fifth, seventh). Individual distortion levels of 2%, 5%, and 8% are considered for each pair of harmonics. In total, 9 harmonic conditions are considered. The final set of supply conditions is obtained by the combination of the voltage unbalance and harmonic distortion values forming a dataset of 3978 unbalanced and distorted voltage conditions (each condition is applied to the motor for 30 seconds). Amongst all conditions, 901 led to a practically constant slip of the motor (slip between 2.4% and 2.6%). They were selected to elaborate Fig. 5, which shows PF_1^g, PF^e, PF_1^a and PF_1^+ as a function of VUF.

In Fig. 5, it can be seen that the TIM 3Φ PFs have a more scattered pattern compared to the correspondent PFs in Fig. 3. This scattering shows that the points obtained experimentally do not superimpose as perfectly as in Fig. 3, meaning that more supply conditions lead to results with the same VUF but different PF values. In Fig. 5, it can be seen that PF^e and PF_1^a definitions presented the greatest scattering bands for any fixed VUF. In other words, PF^e and PF_1^a are the most vulnerable definitions to the unbalanced and distorted conditions. Although all PF definitions present some sensitivity to the presence of unbalances and distortions, one can see that the general behavior of the PFs with respect to VUF is similar in Figures 5 and 3. It can be observed that, when the VUF increases, the scattering band of PF^e and PF_1^a shifts down, the PF_1^g band shifts down slightly, and that the position of the band of PF_1^+ is the most stable presenting the least variation with respect to changes of VUF. In particular, considering the worst case, it can be seen that, for any VUF, the lower values of PFs are such that $PF_1^+ \geq PF_1^g \geq PF_1^a \geq PF^e$. Based on these results, it can be concluded that the experimental investigation and the simulation study are in accordance. Besides, these results indicate that the most recommendable PF definitions for revenue purposes are PF_1^+ and PF_1^g.

VI. EVALUATION OF THE EFFECTS OF MEASUREMENT ALGORITHMS ON THE FAIREST POWER FACTOR DEFINITIONS

This section evaluates the accuracy of the measurement methods discussed in Section III-B considering unbalanced and nonsinusoidal voltage and current signals in conditions with noise and also in conditions without noise. Here, a meter is simulated as an algorithm that measures a specific PF definition. For evaluation, the algorithms should obtain measurements for PF_1^g and PF_1^+ submitted to the same supply and load conditions simulated in Section IV. It is important to note that PF_1^+ must be distinguished as PF_1^{+a} and PF_1^{+g} since they may provide different values, depending on the measurement algorithm applied.

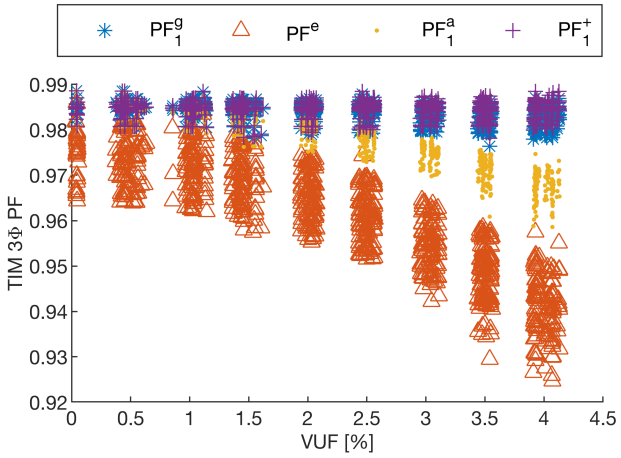

FIGURE 5. Different 3ϕ PF definitions computed for the TIM as a function of the VUF with experimental data (THD values of 2%, 5%, and 8%).

A. ACCURACY OF MEASUREMENT ALGORITHMS: WITHOUT NOISE

In order to evaluate the measurement accuracy as a function of the VU, the error (ΔPF) is computed as the difference between the PF measurement ($PF_{\text{meas.}}$) and the $PF_{\text{ref.}}$. In particular, the error for PF_1^g is

$$\Delta PF_1^g = PF_{1,\text{meas.}}^g - PF_{\text{ref.}}, \tag{25}$$

the error for PF_1^{+a} is

$$\Delta PF_1^{+a} = PF_{1,\text{meas.}}^{+a} - PF_{\text{ref.}}, \tag{26}$$

and the error for PF_1^{+g} is

$$\Delta PF_1^{+g} = PF_{1,\text{meas.}}^{+g} - PF_{\text{ref.}}, \tag{27}$$

where $PF_{1,\text{meas.}}^g$ is computed substituting P and Q by P_1 and Q_1 in (8); $PF_{1,\text{meas.}}^{+a}$ is computed substituting P, S_A, S_B and S_C by P_1^+, S_{1A}^+, S_{1B}^+ and S_{1C}^+ in (7); and $PF_{1,\text{meas.}}^{+g}$ is computed substituting P and Q by P_1^+ and Q_1^+ in (8).

In this simulation, voltage and current waveforms are generated for each VU condition. Then, each signal is sampled 64 times per cycle. A window of calculations of 1s is employed. In the case of positive sequence components, values in the first cycle are not taken into account since the estimation process is only possible after two-thirds of a cycle.

The harmonic active power is often negligible with respect to the total fundamental active power [12], [54]. So, P_1 is measured applying (18). Similarly, P_1^+ is measured with (19). The fundamental reactive power is computed by the 90° displacement of voltage (20) and by the voltage integration (21) methods. The computation of PF_1^{+a} can be simplified taking into account that

$$S_{1A}^{+a} = S_{1B}^{+a} = S_{1C}^{+a} = V_1^+ I_1^+ \tag{28}$$

where V_1^+ and I_1^+ are the fundamental positive sequence voltage and current, respectively. To measure V_1^+ and I_1^+, the instantaneous positive sequence components are estimated and the fundamental component is obtained applying the FFT.

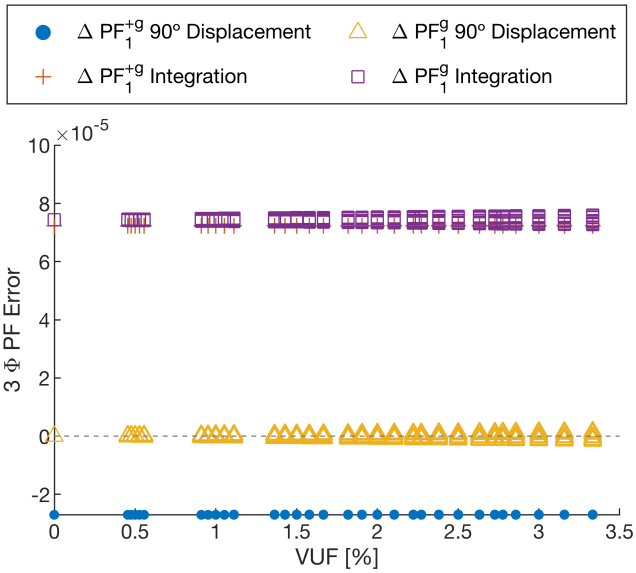

FIGURE 6. ΔPF_1^{+g} and ΔPF_1^{g} with 90° voltage displacement and voltage integration measurement methods for the constant impedance load with simulated data (THD of 3.74%).

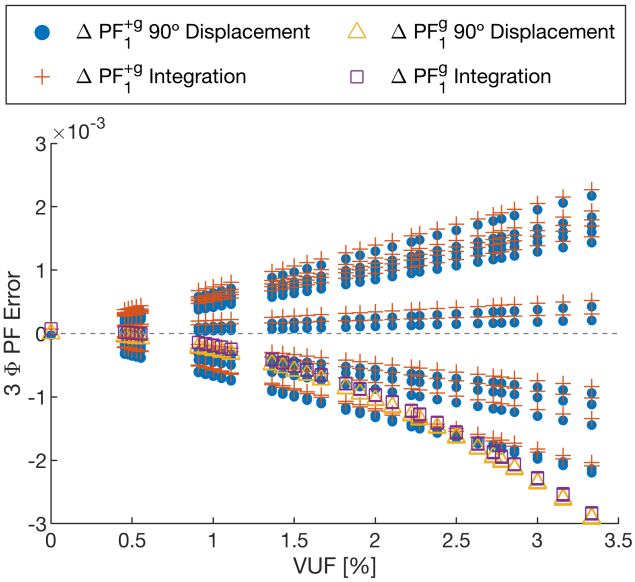

FIGURE 7. ΔPF_1^{+g} and ΔPF_1^{g} with 90° voltage displacement and voltage integration measurement methods for the TIM with simulated data (THD of 3.74%).

Proceeding this way, the values of ΔPF_1^{+a} obtained in the simulation were lower, in module, than 0.0003 and were approximately constant with regard to the VUF.

Fig. 6 shows ΔPF_1^{g} and ΔPF_1^{+g} for the constant impedance load obtained by the 90° displacement of voltage and by the voltage integration techniques as function of VUF. From Fig. 6, it is possible to verify small errors (of order 10^{-5}) for both measurement methods.

Fig. 7 shows ΔPF_1^{g} and ΔPF_1^{+g} for the TIM obtained by the 90° displacement of voltage and by the voltage integration techniques as function of VUF. From Fig. 7, it is possible to verify small errors (of order 10^{-3}) for both measurement methods. Errors of order 10^{-3} are negligible within the existing regulations discussed in Section II.

It can also be observed that for VUF equal to zero, both techniques had deviations close to zero. On the other hand, for a 3% VUF, the methods applied to obtain PF_1^{+g} presented errors from -2×10^{-3} up to $+2\times10^{-3}$, depending on the VU condition. As a matter of fact, PF_1^{+g} reading presented different errors for the same VUF (greater than zero) depending on the condition. This phenomenon is noted to be intensified proportionally to the increase of VUF. This behaviour was not verified for PF_1^{g}. On the other hand, PF_1^{g} readings deviate negatively from its reference value reaching up to -3×10^{-3} for VUF equal to 3.4%. For VUF greater than 2.5%, PF_1^{g} readings performed worst than PF_1^{+g}.

B. ACCURACY OF MEASUREMENT ALGORITHMS: WITH NOISE

In this subsection, it is evaluated how the measurement methods perform with noisy voltage and current signals. For this purpose, an additive white Gaussian noise with standard deviation of 0.2 pu was considered in the signals used in the previous subsection.

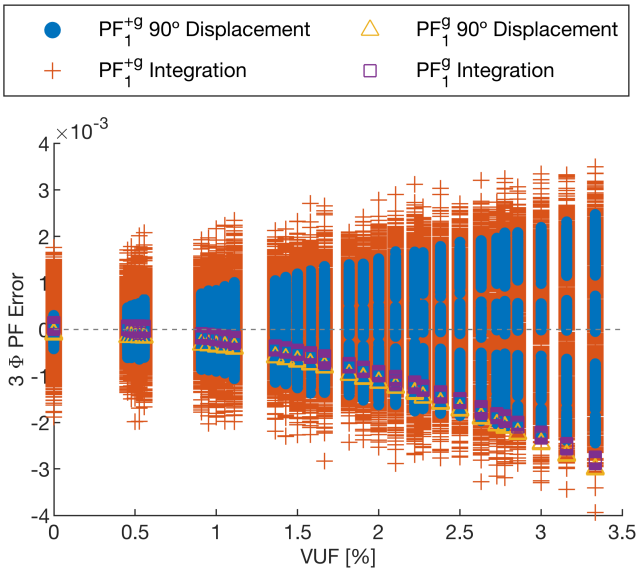

FIGURE 8. ΔPF_1^{+g} and ΔPF_1^{g} measured with the 90° voltage displacement and voltage integration methods for the TIM considering noisy voltage and current signals of simulated data (THD of 3.74%).

The values of ΔPF_1^{+a} obtained with noise were approximately constant (lower, in module, than 0.0003) with regard to the VUF. Therefore, the computation of PF_1^{+a} with the FFT is shown to be robust to the presence of noise in the voltage and current signals.

Fig. 8 shows, as a function of the VUF, the measurement errors of the TIM PF_1^{+g} and PF_1^{g} employing the 90° displacement of voltage and the voltage integration methods. It can be seen that the values of ΔPF_1^{g} measured with both methods are approximately equal to the obtained in Fig. 7. Therefore, the usage of the 90° displacement of voltage and the voltage

integration for measuring PF_1^g is shown to be robust to the presence of noise in the voltage and current signals.

Despite the results of PF_1^{+g} evaluations with the 90° displacement of voltage or the voltage integration methods being sensitive to noise, the maximum and minimum errors are similar to those obtained under noiseless conditions (of order 10^{-3}). Therefore, both PF_1^g and PF_1^{+g} can be accurately measured by the investigated methods considering voltage and current signals with noise up to 0.2 pu.

VII. CONCLUSION

This paper evaluated three-phase PF definitions and their applicable measurement algorithms under several unbalanced and nonsinusoidal voltage conditions.

Simulations showed that all investigated definitions and algorithms yielded fair PF measurements for the balanced constant impedance load. For the motor, billing of PF per phase leads to unfair PF values. For VUF equal or greater than 1.5%, at least one of the phases had a PF value lower than the commonly accepted value of 0.92. It is noteworthy that, in this case, the customer may be penalised due to the voltage unbalance, while the utility has no obligation to improve the supply quality. Among the investigated three-phase definitions, only PF_1^g and PF_1^+ had stable PF readings regardless of the unbalanced or/and nonsinusoidal voltages in simulation and experimental tests.

Additionally, PF_1^g and PF_1^{+g} have the property of being accurately measurable even considering 20% of noise in the voltage and current signals, and employing simple methods such as the 90° displacement and voltage integration methods. In other words, the measured values of PF_1^g and PF_1^{+g} for balanced customers (modeled as constant impedance or as induction motors) have little sensibility on the measurement algorithm and are not affected even if the utility delivers unbalanced nonsinusoidal voltages.

The results obtained in this paper showed that the voltage unbalance and harmonic distortion can reduce the customer's PF^e to values below the acceptable limits. Therefore, the PF^e definition is not the most adequate for the scenarios investigated in this work, even though it is recommended by IEEE Standard 1459-2010. This unexpected conclusion is one of the paper's main contributions and shows that finding the most appropriate PF definition demands more investigation, especially considering situations in which the voltage and the load are both unbalanced.

Considering that PF billing policies impact customers, utilities, and energy meter companies, we suggest, for future works, analysis of the PF and reactive power definitions and measurement methods considering several combinations of supply conditions (unbalanced, nonsinusoidal, etc.) and nonlinear or/and unbalanced loads. Field investigation of commercial meters and of industries bills is also an interesting topic for further research.

ACKNOWLEDGMENT

The authors are grateful to Guilherme Zanetti Rosa and Marcos Diego de Castro e Silva for their valuable assistance in developing the experimental part of this paper.

REFERENCES

[1] M. B. Hughes, "Electric power measurements—A utility's perspective," in *Proc. IEEE Power Eng. Soc. Summer Meeting*, vol. 3, Jul. 2002, pp. 1680–1681, doi: 10.1109/PESS.2002.1043676.

[2] A. J. Berrisford, "Smart meters should be smarter," in *Proc. IEEE Power Energy Soc. Gen. Meeting*, Jul. 2012, pp. 1–6, doi: 10.1109/PESGM.2012.6345146.

[3] *Definitions for the Measurement of Electric Power Quantities Under Sinusoidal, Nonsinusoidal, Balanced, or Unbalanced Conditions*, IEEE Standard 1459, 2010, doi: 10.1109/IEEESTD.2010.5439063.

[4] D. Vieira, R. A. Shayani, and M. A. G. de Oliveira, "Reactive power billing under nonsinusoidal conditions for low-voltage systems," *IEEE Trans. Instrum. Meas.*, vol. 66, no. 8, pp. 2004–2011, Aug. 2017, doi: 10.1109/TIM.2017.2673058.

[5] C.-J. Wu, C.-P. Huang, T.-H. Fu, T.-C. Zhao, and H.-S. Kuo, "Power factor definitions and effect on revenue of electric arc furnace load," in *Proc. Int. Conf. Power Syst. Technol.*, vol. 8. Kunming, China, 2002, pp. 93–97.

[6] S. Pajic and A. E. Emanuel, "Modern apparent power definitions: Theoretical versus practical approach—The general case," *IEEE Trans. Power Del.*, vol. 21, no. 4, pp. 1787–1792, Oct. 2006, doi: 10.1109/TPWRD.2006.876647.

[7] S. Pajic and A. E. Emanuel, "Effect of neutral path power losses on the apparent power definitions: A preliminary study," *IEEE Trans. Power Del.*, vol. 24, no. 2, pp. 517–523, Apr. 2009, doi: 10.1109/TPWRD.2009.2014481.

[8] J. L. Willems, J. A. Ghijselen, and A. E. Emanuel, "The apparent power concept and the IEEE standard 1459–2000," *IEEE Trans. Power Del.*, vol. 20, no. 2, pp. 876–884, Apr. 2005, doi: 10.1109/TPWRD.2005.844267.

[9] A. E. Emanuel, "Apparent power definitions for three-phase systems," *IEEE Trans. Power Del.*, vol. 14, no. 3, pp. 767–772, Jul. 1999, doi: 10.1109/61.772313.

[10] A. E. Emanuel, "The Buchholz-Goodhue apparent power definition: The practical approach for nonsinusoidal and unbalanced systems," *IEEE Trans. Power Del.*, vol. 13, no. 2, pp. 344–350, Apr. 1998, doi: 10.1109/61.660900.

[11] A. E. Emanuel, "On the definition of power factor and apparent power in unbalanced polyphase circuits with sinusoidal voltage and currents," *IEEE Trans. Power Del.*, vol. 8, no. 3, pp. 841–852, Jul. 1993, doi: 10.1109/61.252612.

[12] A. E. Emanuel, "Summary of IEEE standard 1459: Definitions for the measurement of electric power quantities under sinusoidal, nonsinusoidal, balanced, or unbalanced conditions," *IEEE Trans. Ind. Appl.*, vol. 40, no. 3, pp. 869–876, May 2004, doi: 10.1109/TIA.2004.827452.

[13] L. S. Czarnecki and P. M. Haley, "Power properties of four-wire systems at nonsinusoidal supply voltage," *IEEE Trans. Power Del.*, vol. 31, no. 2, pp. 513–521, Apr. 2016, doi: 10.1109/TPWRD.2015.2463253.

[14] M. Faccio and M. Gamberi, "Energy saving in case of intermittent production by retrofitting service plant systems through inverter technology: A feasibility study," *Int. J. Prod. Res.*, vol. 52, no. 2, pp. 462–481, Jan. 2014, doi: 10.1080/00207543.2013.832840.

[15] N. Mbuli and J. H. C. Pretorius, "Some considerations for designing a reactive power charge," in *Proc. Asia–Pacific Power Energy Eng. Conf.*, Mar. 2012, pp. 1–4, doi: 10.1109/APPEEC.2012.6307251.

[16] BC-Hydro. (2017). *Electric Tariff*. [Online]. Available: https://www.bchydro.com/index.html

[17] Hydro-Quebec. (2019). *Electricity Rates*. [Online]. Available: https://www.hydroquebec.com/residential/

[18] Essential Services Commission. (2018). *Victorian Electricity Distribution Code*. Melbourne, Australia. [Online]. Available: https://www.esc.vic.gov.au/

[19] Ergon Energy. (2019). *Network Tariff Guide*. [Online]. Available: https://www.ergon.com.au/

[20] State of Queensland. (2006). *Queensland Electricity Regulation*. [Online]. Available: https://www.commerce.wa.gov.au/

[21] Synergy. (2019). *Standard Electricity Prices and Charges*. [Online]. Available: https://www.synergy.net.au/

[22] Government of Western Australia and Department of Mines, Industry Regulation and Safety. (2008). *Western Australia Electrical Requirements*. [Online]. Available: https://www.commerce.wa.gov.au/

[23] Southern Electric Power Distribution PLC. (2020). *SEPD DUoS Charging Statements 2020/21*. [Online]. Available: https://www.ssen.co.uk/

[24] Southern Electric Power Distribution PLC. (2019). *Statement of Methodology and Charges for Connection to Southern Electric Power Distribution PLC's Electricity Distribution System*. [Online]. Available: https://www.ssen.co.uk/
[25] O. O. Gas and E. Markets. (2019). *The Distribution Code of Licensed Distributions Network Operators of Great Britain*. [Online]. Available: https://www.dcode.org.uk/
[26] Scottish Power Energy Networks. (2020). *Use of System Charging Statement*. [Online]. Available: https://www.scottishpower.com/
[27] Scottish Power Energy Networks. (2007). *Methodology Statement Detailing the Basis of SP Distribution's Use of System Charges*. [Online]. Available: https://www.scottishpower.com/
[28] Agência Nacional de Energia Elétrica. (2016). *PRODIST-Módulo 8-Qualidade da Energia Elétrica*. [Online]. Available: https://www.aneel.gov.br/
[29] Agência Nacional de Energia Elétrica. (2010). *Resolução Normativa Nº 414/2010*. [Online]. Available: https://www.aneel.gov.br/
[30] Agência Nacional de Energia Elétrica. (2015). *Manual de Controle Patrimonial do Setor Elétrico (MCPSE)*. [Online]. Available: https://www.aneel.gov.br/
[31] J. D. Irwin and R. M. Nelms, *Basic Engineering Circuit Analysis*, 9th ed. Hoboken, NJ, USA: Wiley, 2010.
[32] J. L. Willems, "Reflections on apparent power and power factor in nonsinusoidal and polyphase situations," *IEEE Trans. Power Del.*, vol. 19, no. 2, pp. 835–840, Apr. 2004, doi: 10.1109/TPWRD.2003.823182.
[33] S. Frize, "Active reactive and apparent power in circuits with nonsinusoidal voltage and current," *Elektrotechnische Zeitschrift*, vol. 53, no. 25, pp. 596–599, 1932.
[34] C. I. Budeanu, *Puissances Réactives et Fictives*. Bucharest, Romania: Institut Romain de l'Energte, 1927.
[35] J. L. Willems, "A new interpretation of the Akagi-Nabae power components for nonsinusoidal three-phase situations," *IEEE Trans. Instrum. Meas.*, vol. 41, no. 4, pp. 523–527, Aug. 1992.
[36] L. S. Czarnecki, "Scattered and reactive current, voltage, and power in circuits with nonsinusoidal waveforms and their compensation (power systems)," *IEEE Trans. Instrum. Meas.*, vol. 40, no. 3, pp. 563–574, Jun. 1991, doi: 10.1109/19.87020.
[37] L. S. Czarnecki, "What is wrong with the Budeanu concept of reactive and distortion power and why it should be abandoned," *IEEE Trans. Instrum. Meas.*, vol. IM-36, no. 3, pp. 834–837, Sep. 1987, doi: 10.1109/TIM.1987.6312797.
[38] H. Akagi, Y. Kanazawa, and A. Nabae, "Instantaneous reactive power compensators comprising switching devices without energy storage components," *IEEE Trans. Ind. Appl.*, vol. IA-20, no. 3, pp. 625–630, May 1984, doi: 10.1109/TIA.1984.4504460.
[39] W. Shepherd and P. Zakikhani, "Suggested definition of reactive power for nonsinusoidal systems," *Proc. IEE*, vol. 119, no. 9, pp. 1361–1362, Jul. 1972, doi: 10.1049/piee.1973.0173.
[40] A. Cataliotti, V. Cosentino, and S. Nuccio, "The measurement of reactive energy in polluted distribution power systems: An analysis of the performance of commercial static meters," *IEEE Trans. Power Del.*, vol. 23, no. 3, pp. 1296–1301, Jul. 2008, doi: 10.1109/TPWRD.2008.919239.
[41] P. S. Filipski and P. W. Labaj, "Evaluation of reactive power meters in the presence of high harmonic distortion," *IEEE Trans. Power Del.*, vol. 7, no. 4, pp. 1793–1799, Oct. 1992, doi: 10.1109/61.156980.
[42] D. G. Hart, D. Novosel, and R. A. Smith, "Modified cosine filters," U.S. Patent 6 154 687 A, 1998.
[43] W.-K. Yoon and M. J. Devaney, "Reactive power measurement using the wavelet transform," *IEEE Trans. Instrum. Meas.*, vol. 49, no. 2, pp. 246–252, Apr. 2000, doi: 10.1109/19.843057.
[44] W. K. Yoon and M. J. Devaney, "Power measurement using the wavelet transform," *IEEE Trans. Instrum. Meas.*, vol. 49, no. 2, pp. 246–252, Apr. 1998, doi: 10.1109/19.843057.
[45] R. Langella and A. Testa, "A new algorithm for energy measurement at positive sequence of fundamental power frequency, under unbalanced non-sinusoidal conditions," in *Proc. IEEE Lausanne Power Tech*, vol. 2, Jul. 2007, pp. 1558–1563, doi: 10.1109/PCT.2007.4538547.
[46] A. Cataliotti and V. Cosentino, "A time-domain strategy for the measurement of IEEE standard 1459–2000 power quantities in nonsinusoidal three-phase and single-phase systems," *IEEE Trans. Power Del.*, vol. 23, no. 4, pp. 2113–2123, Oct. 2008, doi: 10.1109/TPWRD.2008.2002642.
[47] A. Cataliotti, V. Cosentino, and S. Nuccio, "A virtual instrument for the measurement of IEEE Std. 1459–2000 power quantities," *IEEE Trans. Instrum. Meas.*, vol. 57, no. 1, pp. 85–94, Jan. 2008, doi: 10.1109/TIM.2007.908625.
[48] M. R. Iravani and M. Karimi-Ghartemani, "Online estimation of steady state and instantaneous symmetrical components," *IEE Proc.-Gener., Transmiss. Distrib.*, vol. 150, no. 5, pp. 616–622, Sep. 2003, doi: 10.1049/IP-GTD:20030779.
[49] J. L. Gonzalez-Cordoba, R. A. Osornio-Rios, D. Granados-Lieberman, R. D. J. Romero-Troncoso, and M. Valtierra-Rodriguez, "Correlation model between voltage unbalance and mechanical overload based on thermal effect at the induction motor stator," *IEEE Trans. Energy Convers.*, vol. 32, no. 4, pp. 1602–1610, Dec. 2017, doi: 10.1109/TEC.2017.2706194.
[50] Y.-J. Wang, "Analysis of effects of three-phase voltage unbalance on induction motors with emphasis on the angle of the complex voltage unbalance factor," *IEEE Trans. Energy Convers.*, vol. 16, no. 3, pp. 270–275, Sep. 2001, doi: 10.1109/60.937207.
[51] G. B. Kliman and H. A. Toliyat, *Handbook of Electrical Motors*, 2nd ed. New York, NY, USA: Taylor & Francis, 2004.
[52] P. Gnacinski, "Windings temperature and loss of life of an induction machine under voltage unbalance combined with over- or undervoltages," *IEEE Trans. Energy Convers.*, vol. 23, no. 2, pp. 363–371, Jun. 2008, doi: 10.1109/TEC.2008.918596.
[53] J. L. Willems, "Budeanu's reactive power and related concepts revisited," *IEEE Trans. Instrum. Meas.*, vol. 60, no. 4, pp. 1182–1186, Apr. 2011, doi: 10.1109/TIM.2010.2090704.
[54] M. D. Kusljevic, "A simultaneous estimation of frequency, magnitude, and active and reactive power by using decoupled modules," *IEEE Trans. Instrum. Meas.*, vol. 59, no. 7, pp. 1866–1873, Jul. 2010, doi: 10.1109/TIM.2009.2030865.

VICTOR P. BRASIL received the B.S. and M.S. degrees in electrical engineering from the University of Brasília, Brazil, in 2017 and 2019, respectively.

Since 2019, he has been working as an Engineer with the National Operator of the Electrical System (in Portuguese, Operador Nacional do Sistema Elétrico—ONS), Brazil. His research interests include renewable energies, distributed energy resources, and power quality.

JOÃO Y. ISHIHARA (Member, IEEE) received the Ph.D. degree in electrical engineering from the University of São Paulo, Brazil, in 1998. He is currently an Associate Professor with the University of Brasília, Brazil. His research interests include robust filtering and control theory and their applications in robotics and power systems.

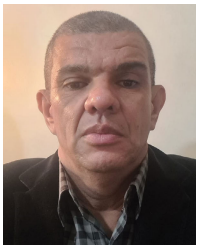

ANÉSIO DE L. FERREIRA FILHO received the Ph.D. degree in electrical engineering from the University of Brasília, Brasília, Brazil, in 2008. He is currently a Professor with the University of Brasília. His research interests include distribution systems, distributed generation, and power quality.